AIMS Materials Science, 8(6): 932–951.
DOI: 10.3934/matersci.2021057
Received: 15 November 2021
Accepted: 13 December 2021
Published: 16 December 2021

http://www.aimspress.com/journal/Materials

Research article

Temperature deformation characteristics of acrylic windows used for tide embankments

Kentaro Yasui[1,*], Akira Shiokawa[2], Masashi Watanabe[3], Hiroyuki Kinoshita[4] and Chihiro Morita[4]

[1] Department of Urban Environmental Design and Engineering, National Institute of Technology, Kagoshima College, 1460-1, Shinko, Hayato-cho, Kirishima, Kagoshima, 899-5193, Japan
[2] Graduate School of Engineering, University of Miyazaki, 1-1, Gakuen-kibanadai-nishi, Miyazaki, Miyazaki, 889-2192, Japan
[3] Nissin Kohgyo Co., Ltd., 74, Honkoji, Nobeoka, Miyazaki, 882-0812, Japan
[4] Faculty of Engineering, University of Miyazaki, 1-1, Gakuen-kibanadai-nishi, Miyazaki, Miyazaki, 889-2192, Japan

* **Correspondence:** Email: yasui@kagoshima-ct.ac.jp; Tel: +81-995-42-9121.

Abstract: Tide-embankment walls protecting coastal roads frequently contain numerous windows so that pedestrians and drivers can view the scenery without experiencing reduced sunlight. Tide-embankment windows must withstand extreme climatic conditions. However, the effects of temperature extremes on acrylic boards have rarely been studied. This paper proposes a simple method for constructing a high-temperature environment and a method for measuring strain on an acrylic plate. The deformation and strain of a 40-mm-thick acrylic tide-embankment window were determined experimentally and numerically in this study in a high-temperature environment, obtaining similar results; additionally, the numerical method was subsequently used to simulate a low-temperature environment. Because thermal conductivity was low, the internal temperature of the thick acrylic board did not immediately change with the temperature of the surface, and thermal expansion and contraction of the board were restrained. Temperature-induced deformation effects were low across the entire range of temperatures and heating rates recorded in coastal Japan.

Keywords: tide-embankment window; acrylic board; high-temperature exposure test; temperature deformation characteristic; finite element analysis

Abbreviations: polymethylmethacrylate (PMMA); autoclaved aerated concrete (AAC); chloroprene rubber (CR)

1. Introduction

Because typhoons and earthquakes occur frequently in Japan [1], concrete tide embankments have been constructed along the coast to prevent storm surges and tsunamis. Although they improve safety, tide embankments can be as high as 5 m, blocking sightlines and sunlight, which deteriorates the quality of the living environment [2,3]. Therefore, slits containing acrylic windows are provided in embankments at regular intervals (Figure 1). Each window consists of a transparent acrylic (polymethylmethacrylate: PMMA) board fitted in a stainless-steel window frame. The window permits a view of the sea or other scenery in normal circumstances but can withstand the water pressure acting on the embankments in the event of a storm surge or tsunami.

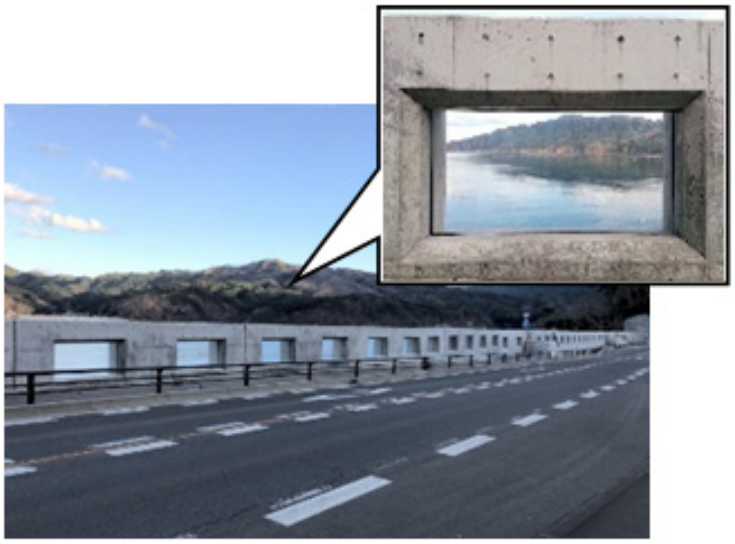

Figure 1. Example of a tide embankment with acrylic windows.

Transparent materials that do not block sightlines and sunlight include acrylic, glass, and polycarbonate. Table 1 presents a comparison of the materials of windows used for tide embankments. Acrylics are the most suitable material for embankment windows because they are hard and strong plastics with excellent optical properties [4] as well as easy to process, lightweight, high bending strength, flexural modulus, and surface hardness; moreover, acrylic boards are not easily scratched [5,6]. Although acrylic windows are currently used for each fixed section of tide embankment constructed along the coast of the Tohoku region in Japan, the effect of the installation environment on the acrylic test pieces has been investigated only for exposure to solar radiation and seawater [7], and the effects of other factors have not yet been clarified. The thickness of the acrylic window used in this study is 40 mm. Although the design is not discussed in this paper, the thickness of 40 mm was determined by examining the thickness that can withstand the hydrostatic pressure due to waves and considering the collision load of drifting objects such as driftwood.

Table 1. Comparison of the materials of the windows used for tide.

Items	Acrylic	Glass	Polycarbonate
Transparency	High (93% or more)	High (92% or more)	High (89% or more)
Density (kg/m^3)	1.19	2.4–2.6	1.20
Impact resistance	High (<polycarbonate)	Low	High (200 times more than glass)
Weather resistance (preserving aesthetics)	Tough	Tough	Aged fading and embrittlement
Processability	High (Cutter cutting)	Difficult (Generally)	Difficult in the field

The focus of the present work is the temperature deformation of acrylic windows installed in an outdoor environment under a wide temperature range. Studies on the temperature-dependent mechanical behavior of acrylic boards have revealed that their elastic modulus, yield stress, and tensile stress decrease with the increase in temperature. However, in a previous study [8], specimens with a total length of 170 mm, width of 10 mm, and thickness of 4 mm were used. Moreover, the tests were conducted under conditions maintained at predetermined temperatures (20 ℃, 40 ℃, 60 ℃, and 80 ℃) [8]. Apparently, the test was not conducted using an acrylic plate with a thickness of 40 mm or in an environment with temperature changes.

The coefficient of linear expansion is commonly used in the study of the temperature deformation of acrylic windows [9,10]; however, this is problematic in the present case: the board used for tide-embankment windows is 40 mm thick and has a thermal conductivity of only 0.21 W/(m·K). Because the board does not easily transfer heat, its surface and interior are unlikely to expand uniformly.

The temperature deformation of an acrylic board has not been experimentally examined. Although heat-conduction analyses of windows in model houses with walls made of autoclaved aerated concrete (AAC), brick, pine, and glass [11] have been performed, there is apparently no examples of analyses with acrylic windows in the literature.

Acrylic boards are used for many applications other than tide embankments, such as display cases, large aquariums [12], and daylighting windows for buildings [13]. Evaluating the temperature deformation of acrylic boards in detail, both experimentally and theoretically, is therefore very important. In the present work, the deformation and strain of a 40-mm-thick acrylic window were measured at high atmospheric temperature. The experimental values were compared with theoretical ones from heat-conduction analysis. The same calculation was performed for the case of a low-temperature environment, which is harder to reproduce experimentally. Because the acrylic window was surrounded by a stainless-steel window frame, the effects of expansion and contraction of acrylic windows on window frame were also examined.

2. Materials and methods

2.1. Experimental specimen and equipment

The experimental specimen was a full-scale acrylic window, as shown in Figure 2a. The dimensions of the window frame were 1160 mm × 2160 mm (opening size 1000 mm × 2000 mm),

and those of the acrylic board were 1060 mm × 2060 mm × 40 mm. The window material used in this study was non-modified cast PMMA board (CLAREX: Nitto Jushi Kogyo Co., Ltd.) in which a polymerization initiator was added to the PPMA and polymerized in a mold. The board was also manufactured in accordance with JIS K6718-1, which is the Japanese Industrial Standard [14]. However, the board thickness range specified by the JIS is 1.5–25 mm; therefore, the thickness of 40 mm for the manufactured board is a custom order.

The experimental equipment shown in Figure 2b was used to provide a high-temperature environment. First, an acrylic window was attached to the fixing stand and installed at the center of the 2400 mm × 2400 mm × 2700 mm thermostat room. The walls of this room were constructed from 40-mm-thick panels of heat insulating material (Styrofoam IB: Du Pont Styro Co., Ltd.) fitted into a wooden frame surrounded by a cedar lumber with a cross-sectional dimension of 45 mm × 45 mm. The inside of the thermostat room was covered with a 2-mm-thick veneer board, and a 4-mm-thick heat shield sheet was attached. Thus, heat forced into the thermostat room from outside using a fan was retained within the room.

A jet heater (HOTGUN125N: Shizuoka Seiki Co., Ltd.) was used to control the temperature inside the thermostat room. Hot air was blown from outside toward a 900 mm × 600 mm vent at the front of the thermostat room. To prevent hot air from directly hitting the acrylic window, a baffle board was installed so that hot air can be evenly distributed in the thermostat room. During the experiment, the temperature was adjusted by varying the distance between the jet heater and thermostat room while checking the temperature inside the latter.

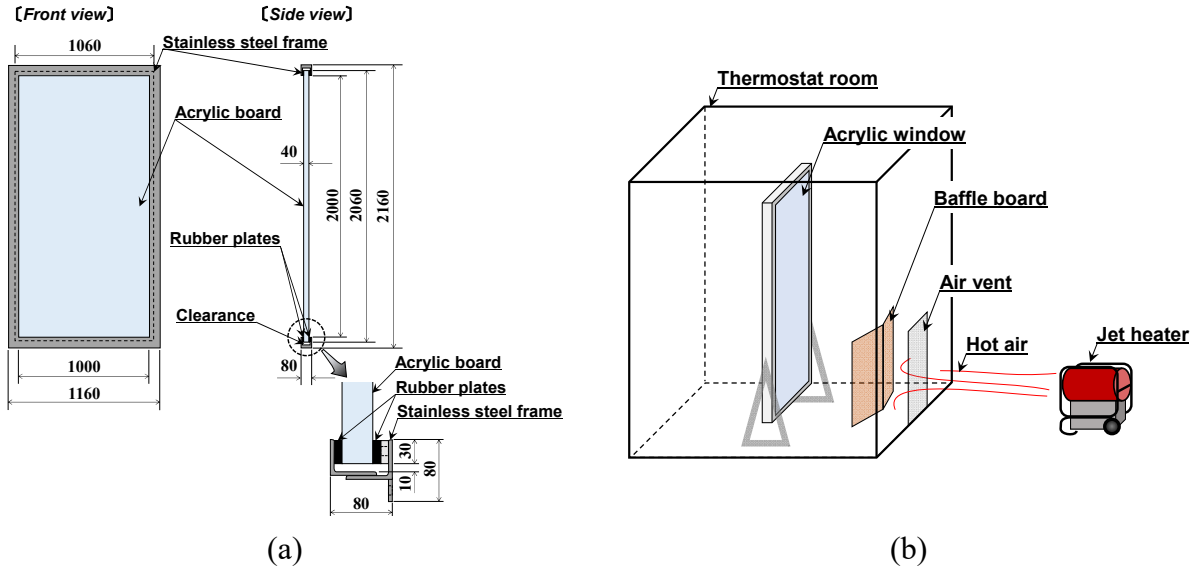

Figure 2. Schematic diagram of acrylic window and experimental equipment. (a) Acrylic window dimensions, (b) Placement of experimental equipment.

2.2. High-temperature environmental conditions

The temperature inside the thermostat room was increased from 10–15 ℃ (the room temperature of the building) to a maximum of 60 ℃. The highest temperature ever observed in Japan (as of the experimental date) was 41.1 ℃ (recorded in Kumagaya City, Saitama Prefecture, on

July 23, 2018) [15]. On that day, the temperature continued to rise for 9 h, from 5:20 am (28.1 ℃) to 2:20 pm. The temperature in our experiment was increased based on these data under the following conditions:

Heating condition 1: 20 ℃/h (increases from 15 to 65 ℃ over 2.5 h);

Heating condition 2: 5 ℃/h (increases from 10 to 60 ℃ over 10 h)

In condition 1, the outside temperature increases so quickly that the interior of the board cannot be expected to follow the sudden temperature change of the acrylic surface, and the strain on the surface will increase. In condition 2, the temperature increases by 50 ℃ over 10 h, comparable to the temperature change in Kumagaya City mentioned above. Although this rate of increase is slower than that of condition 1, the final temperature is 20 ℃ higher than the maximum temperature in Kumagaya City, so this still corresponds to a very harsh thermal environment.

2.3. Displacement and strain measurement method

The acrylic window will expand and deform as the temperature inside the thermostat room increases. The temperature inside the thermostat room, surface temperature of the acrylic window, and displacement of the acrylic window were measured simultaneously to clarify the relationship between temperature and deformation. In addition, the strain acting on the acrylic window was measured using an attached strain gauge; the strain at the edge of the window is expected to be large because the edge of the acrylic window was restrained using a stainless-steel frame lined with chloroprene rubber (CR).

Figure 3 shows the locations of the installed displacement meter, strain gauges, and thermocouples. The displacement in the acrylic plane in Figure 3a was measured by inserting a displacement meter through a hole created in the window frame. The air temperature in the thermostat room in Figure 3b was measured by installing thermocouples at four locations 100 mm from the acrylic window in the out-of-plane direction and averaging their readings. The average value from thermocouples attached to the six acrylic windows was taken as the surface temperature of the windows. The positions of the strain gauges are shown in Figure 3c; some were placed near the window frame where the strain is expected to be larger, whereas some were placed at the center of the acrylic window where the strain is expected to be relatively smaller. A triaxial rosette gauge was installed at the corner of the window. The angle between the vertical and main strains of the triaxial rosette gauges are shown in Figure 3d. The strain was taken to be the average value of the gauges installed at the same location at the front and rear of the window. A data recording device (TDS-530: switch box, ASW-50B; displacement meter, CDP-25; strain gauge, GFLAB-6-70; triaxial rosette gauge, GFRA-3-70; T thermocouple, TG-0.65 (all Tokyo Measuring Instruments Laboratory Co., Ltd.)) was used for the measurements.

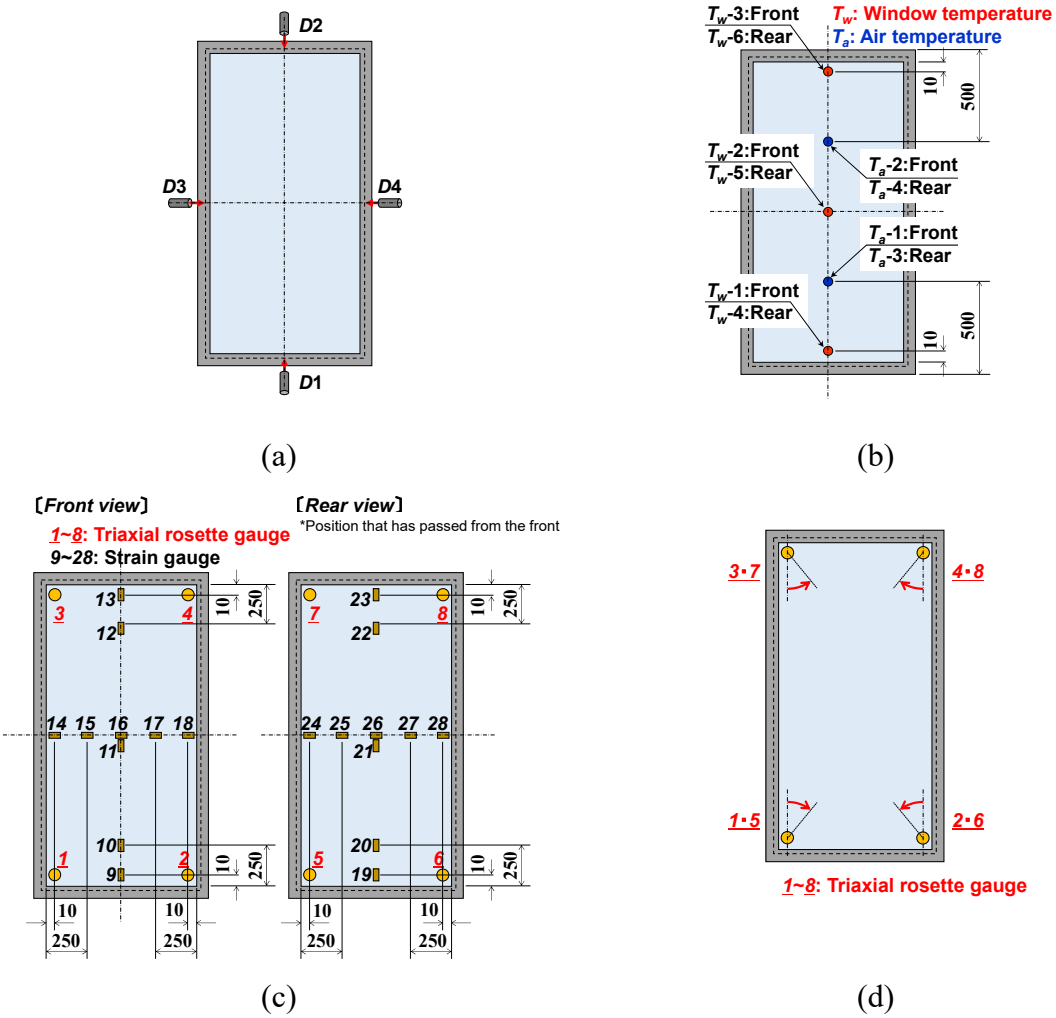

Figure 3. Installation diagram for (a) displacement meters; (b) thermocouples; (c) strain gauges; (d) triaxial rosette gauge, showing the angle between the vertical and main strains.

2.4. Measurable strain of the acrylic windows

It was considered that the strain of the acrylic window consists of three elements (Figure 4). Element 1, the strain due to temperature difference, is caused by the inability of the interior of the acrylic to match the temperature-induced contraction or expansion of the surface because of the thickness and low thermal conductivity of the window (Figure 4a). Element 2, the strain due to external force, is generated when the expansion (contraction) of the acrylic window due to the change in the acrylic surface temperature is restrained by the window frame (CR) (Figure 4b). Element 3, the thermal output (i.e., the difference between the coefficient of linear expansion of the acrylic window and the temperature coefficient of resistance of the strain gauge) is because of free expansion of the experimental specimen and the strain gauge as the temperature increases. Although this strain should theoretically become zero, it does not, because the coefficient of linear expansion differs slightly depending on the type of acrylic material. By measuring the thermal output in

advance and subtracting it from the measured strain, a strain depending only on elements 1 and 2 is obtained. However, this also indicates that the strain due to thermal expansion cannot be measured using a strain gauge.

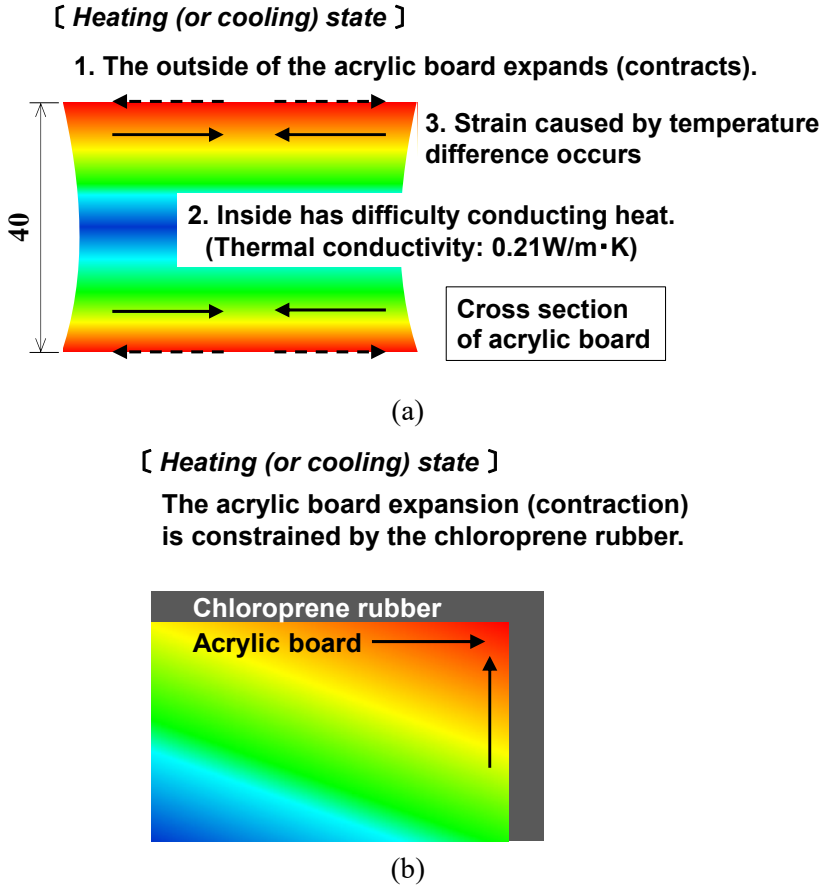

Figure 4. Strain acting on acrylic window: (a) Element 1 (strain due to temperature difference in the cross section of the acrylic board); (b) Element 2 (strain due to restraint force).

2.5. Measurement of thermal output

The thermal output was obtained as follows:

(1) Strain gauges and thermocouples were attached to both sides of a 125 mm × 125 mm × 40 mm acrylic specimen installed in an incubator (KCL-2000A; Tokyo Rika Kikai Co., Ltd.) in an unrestrained state (Figure 5a). The outer circumference of the acrylic specimen was covered with a heat-insulating material to prevent heating and restraint from the incubator.

(2) The temperature inside the incubator was maintained at 20 ℃ for 24 h, to maintain a constant temperature distribution in the thickness direction of the acrylic specimen, and the strain value at that time was set to 0.

(3) The temperature inside the incubator was increased in 5 ℃ increments from 10 to 55 ℃. After 6 h at each incubator temperature, the interior and surface temperatures of the acrylic were equal and the strain value was constant (the thermal output ε_{app}), given to five significant digits by

(see Figure 5b) $\varepsilon_{app} = -0.0001T^4 - 0.0176T^3 - 0.7416T^2 - 5.6528T + 63.985$, where T is the temperature (°C). The strains shown in the results were obtained by subtracting this thermal output from the measured strain.

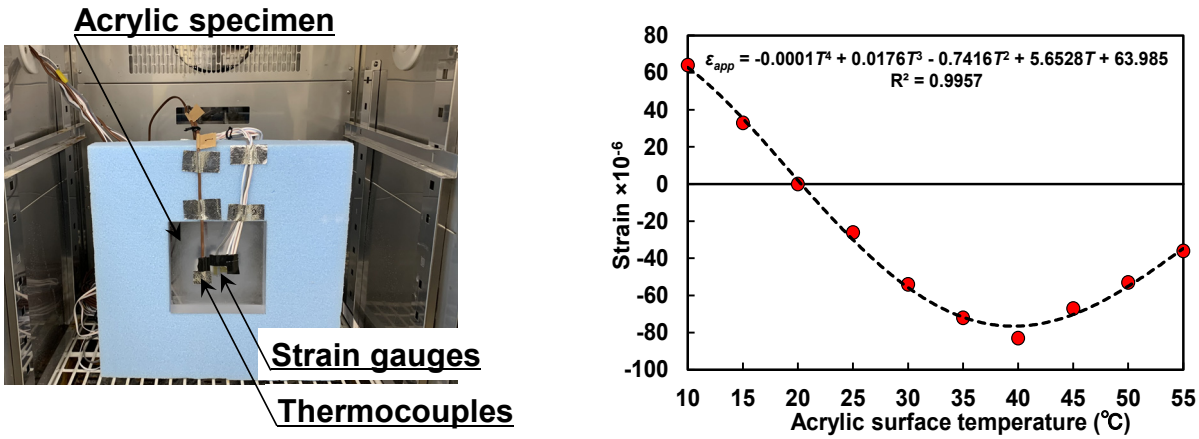

Figure 5. Measurement of thermal output of an acrylic specimen. (a) Acrylic specimen, (b) Thermal output function.

2.6. Analysis conditions

The strain gauge freely expanded as the temperature changed; therefore, it cannot be used to measure the thermal expansion strain of the acrylic window. In addition, it is expected that strain will occur on the surface of the window owing to the temperature difference between the surface and inside; however, the temperature distribution of the window was difficult to measure. Therefore, the thermal-expansion strain and temperature distribution of the acrylic window were calculated using the Marc/Mentat [16] finite element analysis program.

Figure 6 shows a model of the corners of the acrylic and CR. In this analysis, only the acrylic board and the CR that sandwiched it and the window frame were modeled, and 8-node quadrilateral solid elements were used. The element size of the CR was 10 mm × 10 mm × 5 mm; that of the acrylic window was 20 mm × 20 mm × 4 mm, except at the contact area with the CR, where it was 10 mm × 10 mm × 4 mm. The acrylic window and CR were in adhesion contact, so the elements in contact were shared.

The width of the CR in contact with the acrylic window was 30 mm. When the width of the CR in the model was 30 mm, the acrylic window in contact with the CR shared the element. In this case, the deformation of the acrylic window was also constrained by the displacement constraint on the nodal points of the CR. To allow the windows to expand and contract, the width of the modeled CR was set to 40 mm, and the CR protruded 10 mm from the acrylic window.

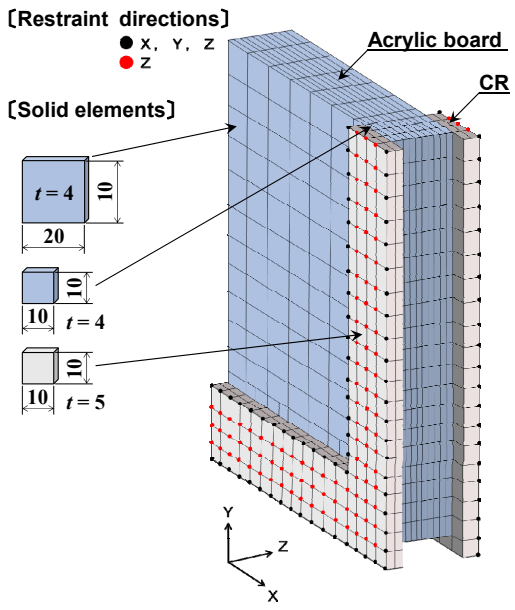

Figure 6. Finite element model of the corners of acrylic board and chloroprene rubber (CR).

Table 2 lists the material properties of acrylic and CR. Because the elastic modulus of acrylic decreases with temperature [17,18] and the linear expansion coefficient of acrylic depends on temperature, the physical properties shown in Figure 7 were used [9].

Table 2. Material properties of acrylic and CR

Properties	Acrylic	CR
Poisson's ratio	0.35	0.49
Density (kg/m^3)	1.19	1.15
Thermal conductivity (W/m·K)	0.21	0.193
Specific heat (kJ/kg·K)	1.5	2.18
Elastic modulus (MPa)	see Figure 7	10
Linear expansion coefficient (1/K)	see Figure 7	0.002

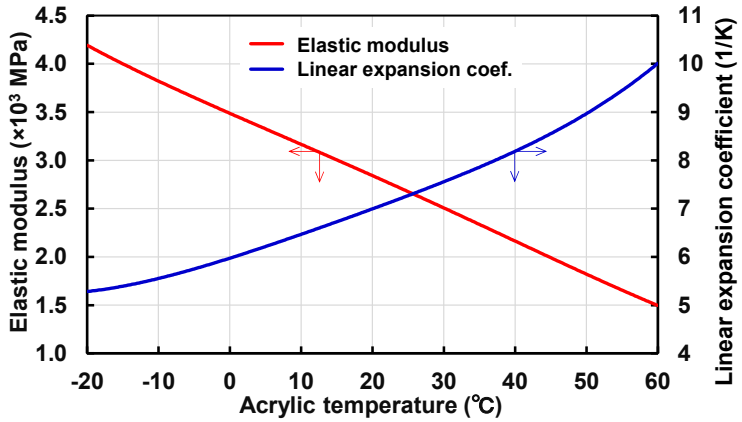

Figure 7. Temperature dependence of plastic modulus and linear expansion coefficient of acrylic.

3. Results and discussion

3.1. Displacement under heating condition 1

Figure 8 shows the measured air temperature, acrylic window surface temperature, and displacement under condition 1. The temperature inside the thermostat room was increased almost constantly at a rate of 20 ℃/h. As the air temperature increased, the acrylic surface temperature also increased, but remained lower than the air temperature, reaching only 50 ℃ when the air temperature exceeded 60 ℃. The surface temperature of the acrylic window decreased when the air temperature decreased.

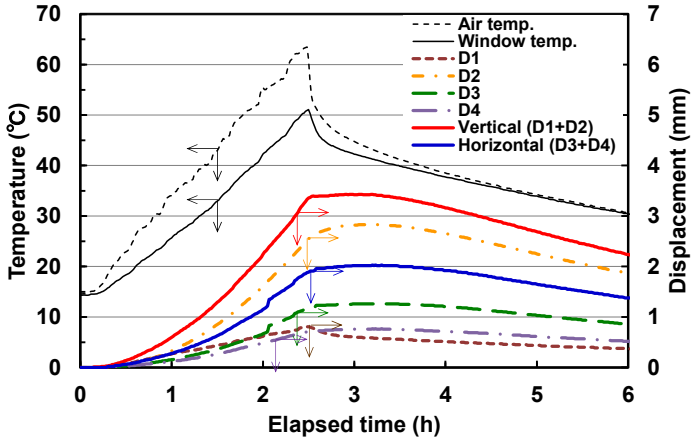

Figure 8. Relationship between air temperature, acrylic-window surface temperature, and displacement in heating condition 1.

The displacement increased with the surface temperature of the acrylic. D2 (i.e., the displacement measured using meter D2 in Figure 3a) was the highest, whereas D1 was the lowest. The two vertical displacements were different because when the acrylic window was installed, its weight acted on the CR between the window frame and the window and the reaction force restricted the expansion of the window. The horizontal displacement D4 was smaller than D3. These four displacements increased slightly, despite the decrease in the surface temperature of the acrylic. At this time, the temperature of the thermostat room reached 60 ℃ and was decreasing. Because the thickness of the acrylic board was 40 mm, the temperature inside the acrylic increased later than that outside, and when the temperature increased, the acrylic expanded.

The maximum values of each displacement were: D1, 0.81 mm; D2, 2.84 mm; D3, 1.26 mm; D4, 0.77 mm. The total displacement in the vertical direction was 3.65 mm, and that in the horizontal direction was 2.03 mm.

3.2. Displacement under heating condition 2

Figure 9 shows the measured air temperature, acrylic window surface temperature, and displacement under condition 2. The temperature inside the thermostat room was increased almost constantly at a rate of 5 ℃/h. As the air temperature increased, the surface temperature of the acrylic

also increased. The difference between the air temperature and the acrylic surface temperature was approximately 5 ℃ (lower than that in Figure 8 because the acrylic surface temperature can follow the slowly changing air temperature).

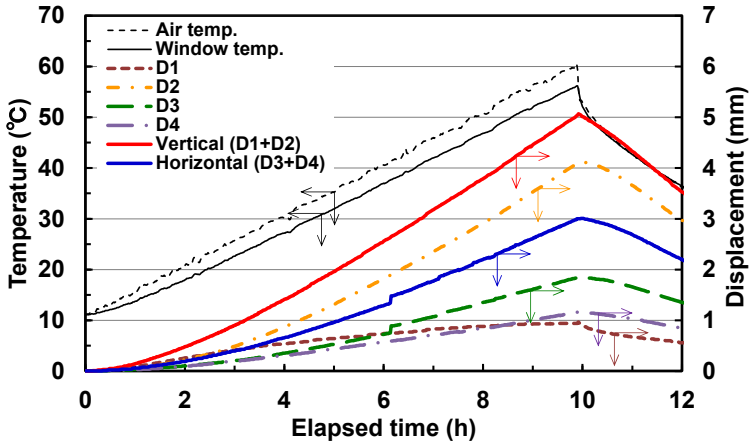

Figure 9. Relationship between air temperature, acrylic-window surface temperature, and displacement in heating condition 2.

The displacement increased as the surface temperature of the acrylic increased. D2 had the highest value, as shown in Figure 8. Under both conditions, D3 was higher than D4 because of the difference in restraint due to the CR between the acrylic and window frame. These deformations reached their maximum values when the air temperature reached 60 ℃ and decreased as the temperature inside the thermostat room and the surface temperature of the acrylic decreased. Because the rate of temperature rise was lower than that under condition 1, the temperature inside the acrylic followed the changing surface temperature of the acrylic to some extent, and the deformation followed accordingly.

The maximum values of each displacement were: D1, 0.97 mm; D2, 4.12 mm; D3, 1.85 mm; D4, 1.16 mm. The total displacement in the vertical direction was 5.09 mm, and that in the horizontal direction was 3.01 mm.

3.3. Strain under heating condition 1

Figure 10 shows the measurement results under heating condition 1 for the acrylic-window surface temperature and the strain in the vertical and horizontal directions of the acrylic window, as well as the main strain at the corner of the acrylic window.

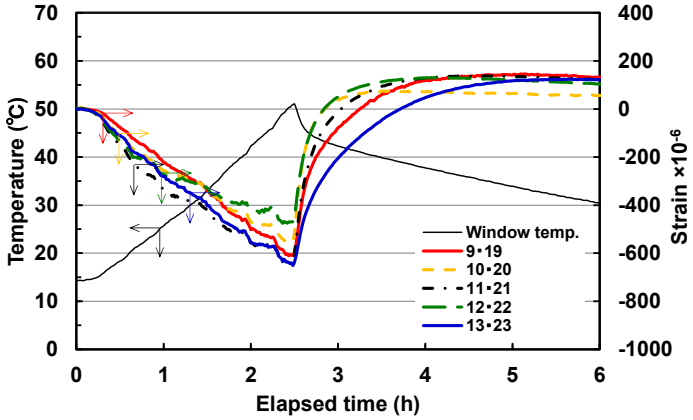

(a)

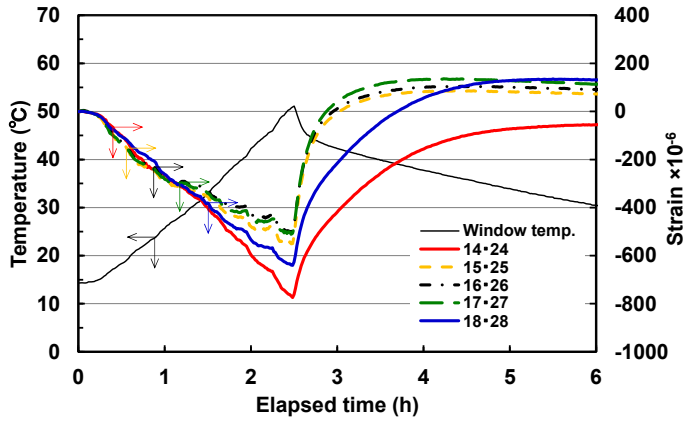

(b)

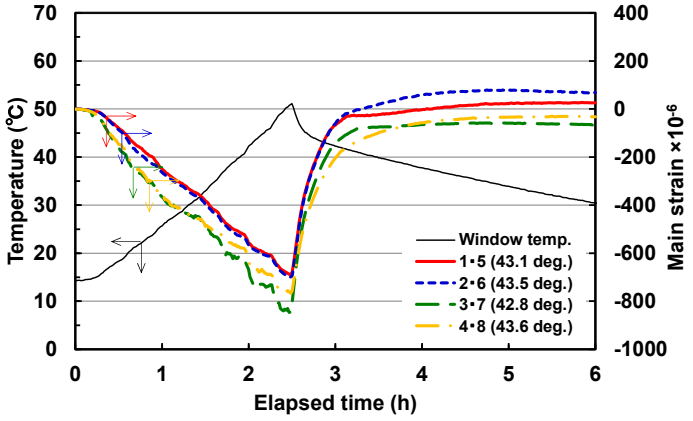

(c)

Figure 10. Acrylic window surface temperature and strain changes over time (heating condition (1) in the (a) vertical direction and (b) horizontal direction. (c) Temperature and main strain at the corner of the window. Numbers identifying the curves refer to strain gauges (Figure 3d) and (in c) to the angle of the main strain from the vertical.

As shown in Figure 10a, compressive strain occurred at all strain gauge attachment points as the surface temperature of the acrylic window increased owing to the temperature difference between the

surface and the inside of the acrylic window (element 1, Figure 4a). Specifically, compressive strain was generated on the surface of the acrylic window because the interior of the acrylic, which is a poor conductor of heat, restrained the expansion produced by heating of the surface. When the surface temperature reached its maximum (50 ℃), the strain also reached its maximum absolute value (450–650 μ).

Similarly, in Figure 10b, a maximum compressive strain of 500–800 μ occurred as the surface temperature of the acrylic window increased. In addition, the strain gauges attached near the window frame had slightly higher maximum readings because of the compressive strains due to the restraint force of the CR and the temperature difference between the surface and the interior.

Figure 10c shows the main strain and direction of the main strain from the measured values of the strain gauge attached at the corner of the acrylic window. The main strain increased with the surface temperature of the acrylic window, exhibiting a maximum compressive strain of 700–900 μ. The strain at the upper part of the window frame was higher than that at the lower part because the displacement of the acrylic window shown in Figure 8 was larger than that at the lower part, and the upper part was more restrained by the CR than the lower part. The average angles of the main strain when the window surface temperature increased were 43.1° at measurement points 1 and 5, 43.5° at measurement points 2 and 6, 42.8° at measurement points 3 and 7, and 43.6° at measurement points 4 and 8. Therefore, the acrylic window was evenly restrained by the window frame.

3.4. Strain under heating condition 2

Figure 11 shows the measurement results under heating condition 2 for the acrylic window surface temperature and strain in the vertical and horizontal directions of the acrylic window, as well as the main strain at the corner of the acrylic window.

As shown in Figure 11a, the compressive strain increased with the surface temperature of the window, but this phenomenon occurred only for the first 2 h, after which the compressive strain was nearly flat, except at the bottom of the window. The compressive strain when the surface temperature reached 50 °C was 150–350 μ, which is lower than that under heating condition 1.

Similarly, in Figure 11b, a maximum compressive strain of 150–550 μ occurred because of the increase in the surface temperature of the acrylic window. The values of strain gauges 14 and 24 were particularly high probably because displacement meter 3 installed near these strain gauges had a large displacement (Figure 9) and was therefore largely restrained by the CR.

Figure 11c shows the main strain and direction of the main strain from the measured values of the strain gauge attached at the corner of the acrylic window. The main strain increased with the surface temperature of the window, showing a maximum compressive strain of 250–300 μ. The average angles of the main strain when the acrylic window surface temperature increased were 42.0° at measurement points 1 and 5, 42.5° at measurement points 2 and 6, 42.3° at measurement points 3 and 7, and 44.0° at measurement points 4 and 8. Therefore, the acrylic window can be evenly restrained by the window frame, just as in heating condition 1.

Here, the maximum strain on the surface of the acrylic window was reduced by at least 200 μ (when compared with the result of heating condition 1) by decreasing the rate of temperature rise. The strain decreased because the temperature difference between the surface and the inside of the acrylic surface was smaller.

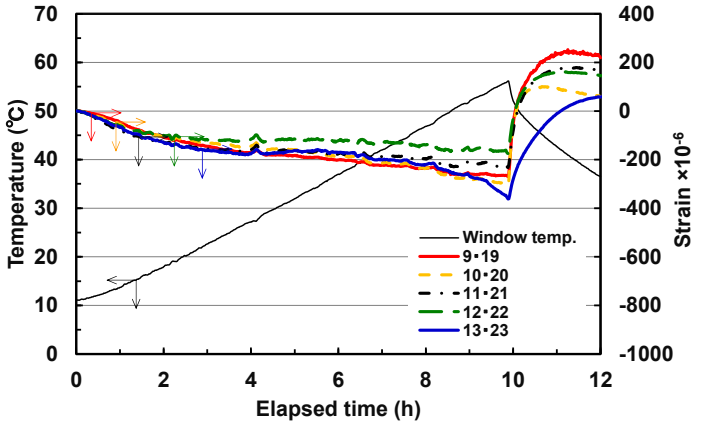

(a)

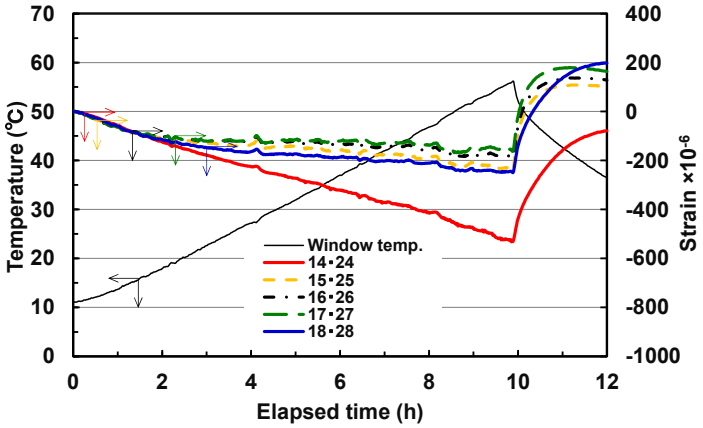

(b)

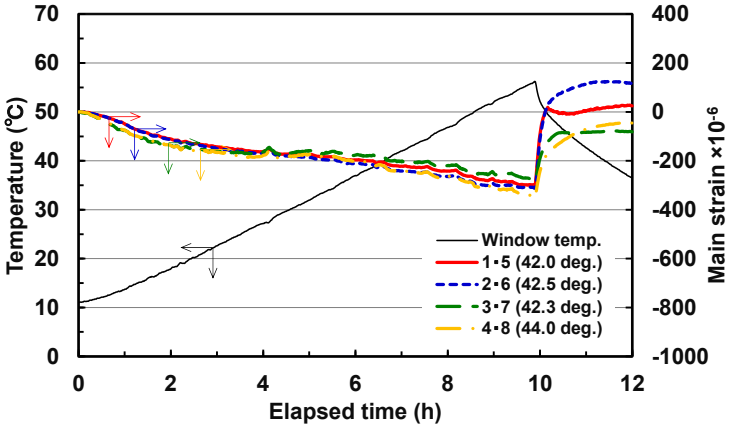

(c)

Figure 11. Acrylic window surface temperature and strain changes over time (heating condition (2) in the (a) vertical direction and (b) horizontal direction. (c) Temperature and main strain at the corner of the window. Numbers identifying the curves refer to strain gauges (Figure 3d) and (in c) to the angle of the main strain from the vertical.

3.5. Temperature-deformation analysis of acrylic windows in a high-temperature environment

The temperature change on the surface of the acrylic window (heating condition 2) shown in Figure 9 was applied to the front and rear of the model, and the acrylic window was analyzed in a high-temperature environment.

Figure 12a shows the relationship between the window surface temperature and the displacement obtained from the analysis. The maximum displacements were 5.38 mm in the vertical direction and 3.22 mm in the horizontal direction. These are almost equal to the values shown in Figure 9 (5.09 mm in the vertical direction and 3.01 mm in the horizontal direction), confirming the validity of the numerical model. Figure 12b,c show the strain and stress distributions due to thermal expansion of the surface of the acrylic window when the surface temperature reached 56.8 ℃, respectively. As the temperature increased, the strain due to thermal expansion also increased. A uniform tensile strain of 3472 μ was generated on the surface of the acrylic window (Figure 12b). This thermal expansion strain is higher than either the strain due to the surface–interior temperature difference or that due to the restraint of CR, as shown in Figure 11.

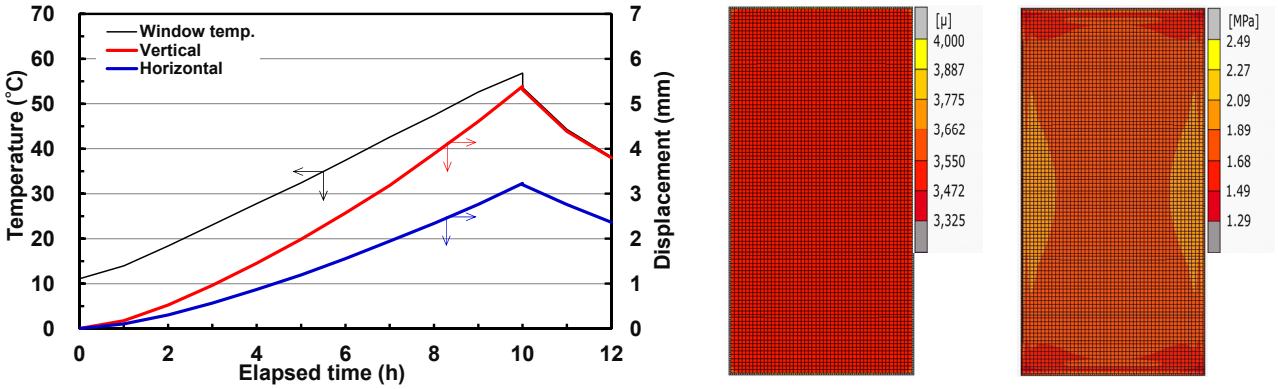

(a) (b) (c)

Figure 12. (a) Relationship between the acrylic window surface temperature and calculated displacement (heating condition 2), (b) strain and (c) stress distributions of the surface of the acrylic window at 56.8 ℃.

In addition, a maximum tensile stress of 2.49 MPa was generated near the middle of the vertical edges of the window frame, as shown in Figure 12c. Because the window was longer in the vertical direction, the displacement due to expansion was also larger in that direction. As the displacement increased, the restraint force from the CR as well as the restraint from the upper and lower surfaces of the window frame also increased. As a result, the stress at the positions farthest from the upper and lower edges of the window frame was the maximum because the compressive stress due to the restraint acted in the direction opposite the tensile stress of the acrylic board. The tensile strength of the acrylic window was 48 MPa (60 ℃) [9]; therefore, the tensile stress generated by thermal expansion was small and had minimal influence on the use of the acrylic window.

3.6. Temperature difference between the surface and interior of the acrylic window

Figure 13a shows the temperature distribution in the thickness direction at a surface temperature of 56.8 ℃. On the horizontal axis of the graph, 0 mm represents the front surface of the acrylic window and 40 mm the position of the rear surface. These front and rear surfaces were both at 56.8 ℃, whereas the central part at a depth of 20 mm from the surface was at 48.8 ℃. Therefore, the maximum temperature difference between the surface and the interior was 8 °C. This resulted in the difference in the temperature-dependent expansion of the acrylic that produced the compressive strain shown in Figure 11.

Figure 13b shows the effect of the temperature difference between the surface and the interior due to the thickness of the acrylic board. The temperature difference at a plate thickness of 40 mm was 8 ℃, whereas it was approximately 17 ℃ at a plate thickness of 60 mm. In contrast, almost no temperature difference occurred when the plate thickness was 10 mm.

This result indicates that the internal temperature difference increased quadratically with respect to the surface temperature as the thickness of the acrylic window increased.

Based on these results, the analysis method can be used in the following cases. The possibility of an earthquake occurring in Nankai Trough, Japan, is high [1]. Hence, tide embarkment constructions are expected to increase, as well as the height. As the tide embankments become higher, the acrylic window may become larger, thereby requiring the board thickness to be increased. By using the analysis method presented in this study, the deformation characteristics of acrylic windows due to temperature change in the construction environment can be predicted and considered in the design.

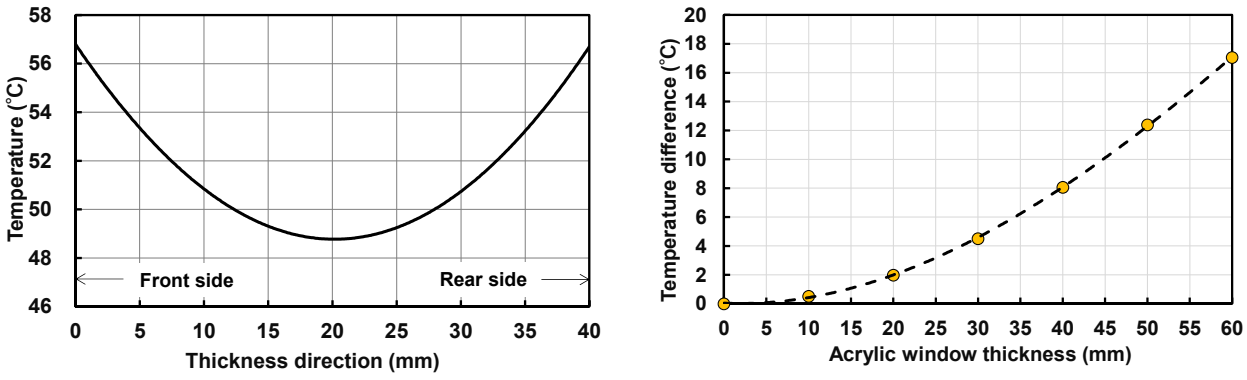

(a) (b)

Figure 13. (a) Temperature distribution in the thickness direction of the acrylic window and (b) temperature difference caused by acrylic window thickness.

Thus, the results of this study will advance the use of acrylic windows and materials in various fields.

3.7. Temperature deformation analysis of acrylic windows in low-temperature environment

An experiment in a low-temperature environment was considered, but it was not possible to

prepare a device to cool the inside of the thermostat room displayed in Figure 2b.

Under the same conditions (except for surface temperature), the properties of the acrylic window were calculated in a low-temperature environment. The coldest conditions recorded in a coastal area of Japan occurred at Watari Town, Miyagi Prefecture, on January 24, 2017 [12]. On that day, the temperature continued to decrease for 15 h, from −0.7 ℃ at 10:00 am to −11.1 ℃ at 1:00 am the next day. Therefore, in this analysis, the temperature deformation was calculated as the surface temperature of the acrylic window decreased from 0 ℃ to −20 ℃ over 15 h.

Figure 14a shows the relationship between the acrylic surface temperature and the calculated displacement. At −20 ℃, the displacements were –1.98 mm in the vertical direction and −1.09 mm in the horizontal; its absolute magnitude increased as the temperature decreased.

Figure 14b,c show the strain and stress distributions due to shrinkage of the surface of the acrylic window when the surface temperature of the acrylic window reached −20 ℃. The thermal-shrinkage strain increased as the temperature decreased, and a uniform compressive strain of 1104 μ was generated, as shown in Figure 14b. In Figure 14c, a very small compressive stress of 0.04 MPa was generated on the entire surface. A slight additional tensile stress was generated near the window frame due to CR restraint.

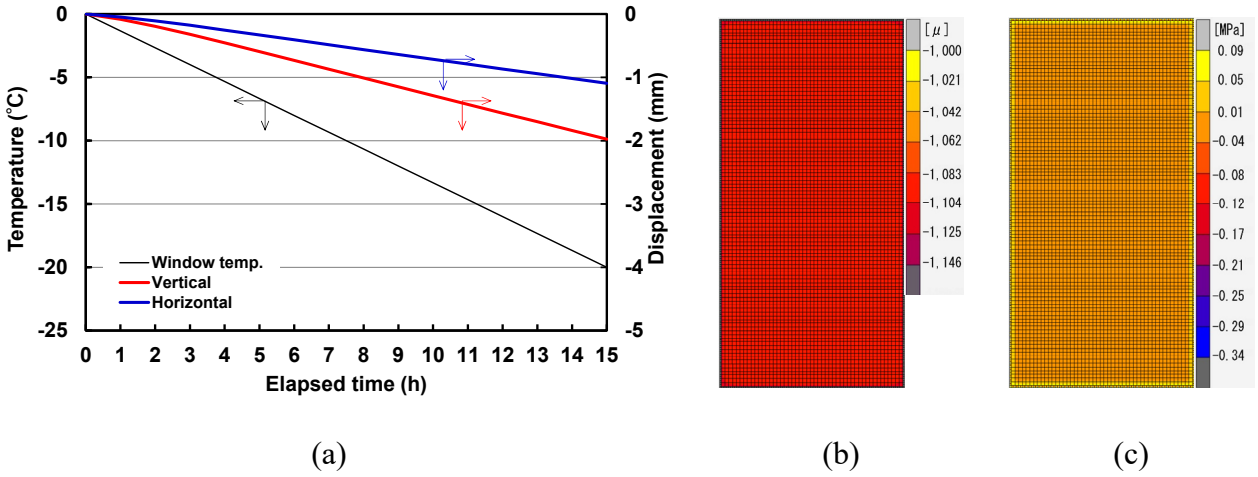

(a) (b) (c)

Figure 14. (a) Relationship between acrylic-window surface temperature and calculated displacement, (b) strain and (c) stress distributions of the surface of the acrylic window at −20 ℃.

3.8. Effect of expansion and contraction of acrylic windows on window-frame mounting

Figure 2a shows a schematic diagram of the connection between the acrylic board and the window frame. The clearance between them was 10 mm on one side, and the entire window frame had a clearance of 20 mm in both the vertical and horizontal directions. A comparison of the maximum in-plane deformations obtained from the experiments and analyses (Table 3) and the clearance indicate that the expansion of the acrylic board was smaller than the clearance on the high-temperature side where the surface temperature of the acrylic window was up to 60 ℃. However, even on the low-temperature side (as cold as −20 ℃), the shrinkage of the acrylic board was significantly smaller than the 30 mm sandwich between layers of CR. From this result, it may be

concluded that, on the one hand, the expanded acrylic board does not exert a large force on the window frame in the high-temperature environment, and, on the other, the contracted acrylic board does not come off from the window frame in the low-temperature environment.

Table 3. Maximum displacement of acrylic board.

Properties	Vertical direction (mm)	Horizontal direction (mm)	Board temp. (℃)
Measured, high-temperature environment, 20 ℃/h	3.65	2.03	56.8
Measured, high-temperature environment, 5 ℃/h	5.09	3.01	
Calculated, high-temperature environment, 5 ℃/h	5.38	3.22	
Calculated, low-temperature environment, –1.3 ℃/h	–1.98	–1.09	–20

4. Conclusions

In this study, changes in the displacement and strain of acrylic windows in a high-temperature environment were measured as the temperature increased to investigate the temperature deformation characteristics of the 40-mm-thick acrylic board used for tide embankments. In addition, a heat conduction analysis was performed to verify the time variations of displacement and strain in high and low-temperature environments. The main findings of this study are summarized below.

(1) In an experiment to reproduce a high-temperature environment, the displacements of the acrylic window in the in-plane direction when the surface temperature exceeded 50 ℃ were 3.65 mm in the vertical direction and 2.03 mm in the horizontal direction under a heating condition of 20 ℃/h. Under a heating condition of 5 ℃/h, the corresponding values were 5.09 mm and 3.01 mm, respectively. Thus, the displacement was smaller at a higher heating rate. Because the acrylic window was thick (40 mm) and the thermal conductivity was low, the internal temperature did not immediately increase with the temperature at the surface of the acrylic window and internal thermal expansion was delayed.

(2) Although the expansion strain cannot be measured using a strain gauge installed at the surface of the acrylic window, the combined strain due to the restraint of the window frame and the temperature difference between the surface and the interior can be obtained. Maximum compressive strains of 800 μ and 550 μ were generated when the temperature increased at the rates of 20 ℃/h and 5 ℃/h, respectively. The strain near the window frame tended to be higher, which increased as the heating rate increased. Because the internal temperature did not immediately increase with the temperature at the surface, the expansion of the surface was restrained.

(3) From the numerical analysis, thermal expansion strain occurred in the acrylic window as the surface temperature increased. This strain was higher than the measured compressive strain due to the CR restraint and the compressive strain due to the temperature difference between the acrylic window surface and the interior. The tensile strain due to thermal expansion was dominant in a high-temperature environment. The maximum tensile stress generated was 2.49 MPa. The tensile strength of the acrylic window was 48 MPa (60 ℃); therefore, the tensile stress caused by thermal expansion is small compared with this value.

(4) The internal temperature difference with respect to the surface temperature increased as the thickness of the acrylic window increased during the analysis.

(5) Numerical analysis of the temperature deformation of acrylic windows with surface temperatures from –20 ℃ to 60 ℃ showed that on the one hand, no force due to the expansion of the acrylic board acted on the window frame, and, on the other, the contracting acrylic board did not come off the window frame.

Acknowledgments

This research did not receive any specific grant from funding agencies in the public, commercial, or not-for-profit sectors.

Conflict of interest

The authors declare that they have no known competing financial interests or personal relationships that could have influenced the research reported herein.

References

1. Earthquakes and Tsunamis—Observation and Disaster Mitigation, Japan Meteorological Agency, 2021. Available from: https://www.jma.go.jp/jma/kishou/books/jishintsunami/en/jishintsunami_en.pdf.
2. Yamashita H (2010) Living together with seawalls: Risks and reflexive modernization in Japan. *Environ Sociol* 6: 161–181.
3. Kimura S (2016) When a seawall is visible: Infrastructure and obstruction in post-tsunami reconstruction in Japan. *Sci Cult* 25: 23–43.
4. Pawar E (2016) A review article on acrylic PMMA. *IOSR J Mech Civ Eng* 13: 1–4.
5. Kishimoto Y (2010) Characteristic and processing method of acrylic resin. *J Measur Subcomm* 18: 24–28 (in Japanese). Available from: https://doi.org/10.18973/measurementjsrt.18.1_24.
6. Harper CA, Petrie EM (2003) *Plastics Materials and Processes: A Concise Encyclopedia*, 1 Ed., New York: John Wiley & Sons, 7–9.
7. Kaddouri A, Serier B, Kaddouri K, et al. (2020) Experimental analysis of the physical degradation of polymers—The case of polymethyl methacrylate. *Frat Integrità Strutt* 14: 66–80.
8. Abdel-Wahab AA, Ataya S, Silberschmidt VV (2017) Temperature-dependent mechanical behaviour of PMMA: Experimental analysis and modelling. *Polym Test* 58: 86–95.
9. Japan Petrochemical Industry Association Methacrylic Policy Committee Technical Working Group (2009) *Design Handbook Using Acrylic Plate* (in Japanese).
10. Shimbo M, Sugimori S, Miyano Y, et al. (1990) Residual stress and deformation of PMMA due to thermoviscoelastic behavior. *Trans JSME* 56: 971–977 (in Japanese). Available from: https://doi.org/10.1299/kikaia.56.971.
11. Siriteerakul S, Siriteerakul T (2017) Heat conduction analysis of wall materials, *Proceedings of the International Conference on Engineering, Science, and Applications*, Tokyo: Global Academic-Industrial Cooperation Society, 1: 63–74.
12. Kohsaka Y (2017) Transformable acrylic resin. *Chem Edu* 65: 236–237 (in Japanese). Available from: https://doi.org/10.20665/kakyoshi.65.5_236.

13. Iduka G (1956) Polymer materials for architecture. *Polymers* 5: 280–283 (in Japanese). Available from: https://doi.org/10.1295/kobunshi.5.6_280.
14. Japanese Industrial Standards (2015) Plastics-poly(methyl methacrylate) sheets-types, dimensions and characteristics-Part 1: Cast sheets. JIS K 6718-1 (in Japanese).
15. Japan Meteorological Agency, Past Weather Data, 2021 (in Japanese). Available from: https://www.data.jma.go.jp/obd/stats/etrn/view/rankall.php.
16. MSC Software Corporation, MARC Volume A Theory and User Information, 2017. Available from: http://www.mscsoftware.com/.
17. The Japan Society for Technology of Plasticity (1991) *Molten and Solid State Molding of Plastics—From Fundamental Phenomena to Advanced Technologies*, 1 Ed., Tokyo: Corona Publishing, 15: 216–217 (in Japanese).
18. Zhou J, Heisserer U, Duke PW, et al. (2021) The sensitivity of the tensile properties of PMMA, Kevlar® and Dyneema® to temperature and strain rate. *Polymer* 225: 123781.

AIMS Press